Available online at www.sciencedirect.com

ScienceDirect

journal homepage: www.elsevier.com/locate/watres

Mechanism, kinetics and toxicity assessment of OH-initiated transformation of triclosan in aquatic environments

Yanpeng Gao [a,b], Yuemeng Ji [a], Guiying Li [a], Taicheng An [a,*]

[a] State Key Laboratory of Organic Geochemistry and Guangdong Key Laboratory of Environmental Resources Utilization and Protection, Guangzhou Institute of Geochemistry, Chinese Academy of Sciences, Guangzhou 510640, China

[b] University of Chinese Academy of Sciences, Beijing 100049, China

ARTICLE INFO

Article history:
Received 5 July 2013
Received in revised form
6 October 2013
Accepted 8 October 2013
Available online 22 October 2013

Keywords:
Phototransformation process
Triclosan
Hydroxyl radical
Theoretical calculation
Risk assessment

ABSTRACT

The mechanisms and kinetics of OH-initiated transformation of triclosan (TCS) in aquatic environments were modeled using high-accuracy molecular orbital theory. TCS can be initially attacked by •OH in two ways, OH-addition and H-abstraction. Twelve OH-addition routes were reported, and the C atom adjacent to the ether bond in the benzene ring ($R_{add}B_1$) was found as the most easily attacked position by •OH, producing •TCS−OH_{B1}. Seven H-abstraction routes were reported, and the •OH exclusively abstracted the phenolic hydroxyl ($R_{abs}OH$) H atom, to form •TCS(−H). The kinetics results showed that the $R_{add}B_1$ and $R_{abs}OH$ routes would occur preferentially in aquatic environments, and the half-life depended on the •OH concentration ([•OH]). At low [•OH], the main intermediates, •TCS −OH_{B1} and •TCS(−H), can be converted into 2,4-dichlorophenol and polychlorinated dibenzo-*p*-dioxins, respectively. However, when enough •OH is present, such as in advanced oxidation process (AOP) systems, they would be fully decomposed. The acute and chronic toxicities of TCS and its products were assessed at three trophic levels using the "ecological structure–activity relationships" program. The toxicity of the products decreased through the $R_{add}B_1$ route, while the toxicity of the products first increased and then decreased through the other degradation routes. These results should help reveal the mechanism of TCS transformation as well as risk assessment in aquatic environments, and will help design further experimental studies and industrial application of AOPs.

1. Introduction

Triclosan (TCS), a member of the class of compounds called pharmaceutical and personal care products, is extensively used in household cleaners, skin care creams, soaps, and toothpastes as a broad-spectrum antimicrobial and preservative agent. It is also frequently used in plastic products, toys, and underwear because of its capacity to inhibit microbial growth. Approximately 1500 t of TCS is produced annually worldwide (Chen et al., 2012), and up to 96% of TCS can be washed down the drain and into the sewerage system during normal use, eventually entering the aquatic environment. Thus, TCS has been classed as an emerging contaminant (EC) (Anger et al., 2013). Although wastewater treatment plants can

* *Corresponding author*. Tel.: +86 20 85291501; fax: +86 20 85290706.
E-mail address: antc99@gig.ac.cn (T. An).

0043-1354/$ – see front matter © 2013 Elsevier Ltd. All rights reserved.
http://dx.doi.org/10.1016/j.watres.2013.10.027

remove more than 90% of TCS through sorption to the solid phase or biodegradation, the residual TCS is unavoidably discharged into the aquatic environment (Heidler and Halden, 2007), and TCS has been detected in wastewater treatment plant effluents (Singer et al., 2002), natural waters (Fair et al., 2009; Kolpin et al., 2002), and various organisms (Allmyr et al., 2006; Calafat et al., 2008; Geens et al., 2012; Liang et al., 2013; Valters et al., 2005; Wilson et al., 2003), including algae, fish, and humans. Furthermore, TCS and its transformation products have been found to be associated with adverse effects on aquatic organisms and to have endocrine-disrupting effects on the mammals (Ishibashi et al., 2004; Raut and Angus, 2010), including causing human breast cancer (Gee et al., 2008). The fate of TCS and its transformation products in the aquatic environment has become of great concern.

Generally, ECs in natural surface waters can be transformed through biodegradation, hydrolysis, and photolysis. However, biodegradation and hydrolysis have been reported to be ineffective for TCS (Singer et al., 2002), and photolysis has been found to be an important TCS transformation process in surface waters (Anger et al., 2013; Kliegman et al., 2013). Therefore, the most important factor controlling the fate of TCS in aquatic environments is likely to be its photolysis (Boreen et al., 2003). However, as well as direct photolysis (Anger et al., 2013; Latch et al., 2003; Wong-Wah-Chung et al., 2007), the phototransformation of TCS includes photosensitized transformation (Wong-Wah-Chung et al., 2007), and reaction with reactive species (RSs). Research in this area has mainly been focused on identifying and quantifying the polychlorinated dibenzo-*p*-dioxin (called "dioxin" in the rest of this paper) photoproducts that can be formed and the transformation pathways in the direct photolysis and photosensitized transformation of TCS (Anger et al., 2013; Kliegman et al., 2013; Latch et al., 2003, 2005; Mezcua et al., 2004; Wong-Wah-Chung et al., 2007). Studies of TCS intermediates or phototransformation mechanisms involving RSs in water, and the natures of the reactions involved, have not yet been published.

A number of RSs, such as •OH, H_2O_2, $^1O_2$, and $CO_3^{\bullet-}$, are formed and are constantly present at low concentrations in natural waters (Dong and Rosario-Ortiz, 2012; Vione et al., 2006). Of these, •OH is a well-known highly reactive oxidant that plays an important role in the transformation of a wide spectrum of ECs in natural waters (Dong and Rosario-Ortiz, 2012; Wenk et al., 2011) because of the high absolute bimolecular rate constants with ECs (An et al., 2010a, 2010b; Buxton et al., 1988; Fang et al., 2013; Yang et al., 2010). High •OH concentrations can be produced easily under certain extreme conditions, for example in advanced oxidation process (AOP) systems (An et al., 2010a, 2010b; Bokare and Choi, 2011; Fang et al., 2013; Shu et al., 2013; Yang et al., 2010). OH-initiated reactions with ECs are, therefore, likely to occur in aquatic environments (either natural waters or AOP systems), regardless of the aquatic conditions. However, all published studies on TCS transformation mechanisms and kinetics up to now have been conducted using photocatalytic experimental systems (Rafqah et al., 2006; Son et al., 2009; Yu et al., 2006), and there are no published studies using a theoretical approach. Furthermore, the potential risks posed by most (~99%) of the transformation products have not been fully considered because the products have not been identified experimentally (Aranami and Readman, 2007), although dioxin-type intermediates have been identified during the phototransformation of TCS.

In this work, to better understand the fate of, and to fully assess the potential risks posed by, TCS in the aquatic environment, the mechanisms and kinetics for OH-initiated transformation of TCS were systematically investigated using the quantum chemical approach. The TCS transformation mechanisms and the causes of different intermediates being produced were elucidated using theoretical calculations, and the possibility of dioxins being formed was assessed under different OH-initiated reaction conditions. The potential risks posed by TCS and its transformation products were also evaluated theoretically using a high-throughput computational tool, the "ecological structure–activity relationships" (ECOSAR) program. The theoretical data obtained can complement experimental results and allow researchers to properly estimate the potential risks posed by TCS and its transformation products in the aquatic environment.

2. Computational methods

2.1. *Electronic structure calculations*

All quantum chemical calculations were performed using the Gaussian 03 program (Frisch et al., 2003). The geometries of all stationary points were optimized using the hybrid density functional B3LYP method with the 6-31+G(d,p) basis set, B3LYP/6-31+G(d,p). Harmonic vibrational frequencies were calculated at the same level to identify all stationary points as either minima (zero imaginary frequency) or transition states (TSs; only one imaginary frequency), and to provide the thermodynamic contributions to the free energy. Intrinsic reaction coordinate calculations were conducted to confirm that each TS really connected the corresponding reactants with the products. Single point energies, including the solvent effect, were calculated using the B3LYP/6-311++G(3df,2p), based on the optimized structures described above, and the conductive polarizable continuum model (Barone and Cossi, 1998) was used to assess the solvent effect.

In solution, the mechanisms involving single-electron transfer can be possible and calculated using Macurs theory (Marcus, 1964, 1993, 1997). The activation barrier ($\Delta G^{\neq}_{Tran}$) is defined in terms of the free energy of reaction (ΔG^{0}_{Tran}) and the nuclear reorganization energy (λ):

$$\Delta G^{\neq}_{Tran} = \frac{\lambda}{4}\left(1 + \frac{\Delta G^{0}_{Tran}}{\lambda}\right)^2 \quad (1)$$

Reorganization energy (λ) has been calculated as

$$\lambda = \Delta E_{Tran} - \Delta G^{0}_{Tran} \quad (2)$$

where ΔE_{Tran} has been calculated as the nonadiabatic energy difference between reactants and vertical products. This approach is similar to the one previously used by Nelsen and co-workers for a large set of single-electron transfer reactions (Nelsen et al., 1987, 2006).

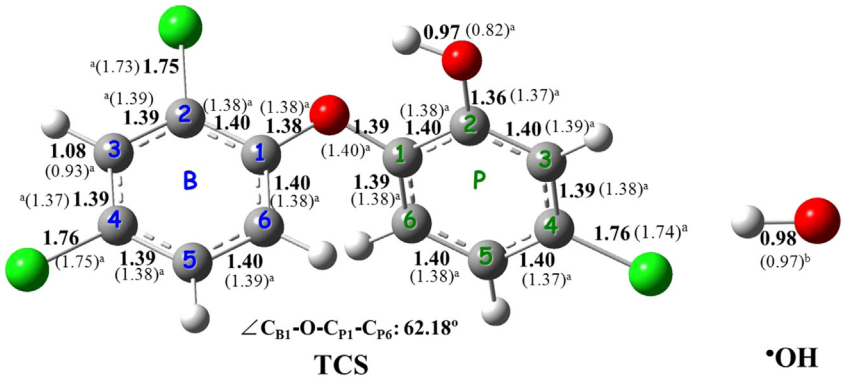

Fig. 1 – The optimized geometries for the reaction of triclosan with •OH at the B3LYP/6-31+G(d,p) level. The values in parentheses are experimental data from the reference of Latosińska et al. (2012) [a], and NIST, 2013[b]. Bond lengths are in Å, ● = C, ● = H, ● = O, ●=Cl.

2.2. Reaction kinetics calculations

Using the above potential energy surface information, the reaction kinetics were calculated using conventional transition state theory (TST) as follows (Galano and Alvarez-Idaboy, 2009; Eyring, 1935; Evans and Polanyi, 1935):

$$k = \sigma \frac{k_B T}{h} \exp\left(\frac{-\Delta G^{\neq}}{RT}\right) \quad (3)$$

In the Eq. (3), k_B and h are the Boltzmann and Planck constants respectively; $\Delta G^{\neq}$ is the free energy barrier including the thermodynamic contribution corrections; σ represents the reaction path degeneracy, accounting for the number of equivalent reaction paths.

In addition, to simulate realistic conditions in the solution, the solvent cage effect is considered according to the correction proposed by Okuno (1997) and took into account the free volume theory. The expression used to correct Gibbs free energy as follows:

$$\Delta G_S^{FV} \cong \Delta G_S^0 - RT\{\mathrm{Ln}[n10^{(2n-2)}] - (n-1)\} \quad (4)$$

where n represents the molecule number of the reaction. According to Eq. (4), the contribution of cage effects was considered and the Gibbs free energy data decreased by 2.54 kcal/mol for bimolecular reactions at 298.15 K.

Some of the calculated rate constant (k) values are found to be close to the diffusion-limit. Thus, in the present work, the Collins-Kimball theory as shown in Eq. (5) was employed to consider the effect of diffusion-limit based on TST calculations (Collins and Kimball, 1949):

$$k_{app} = \frac{kk_D}{k + k_D} \quad (5)$$

where k is the thermal rate constant, obtained from TST calculations from Eq. (3), and k_D is the steady-state rate constant for an irreversible bimolecular diffusion-controlled reaction. And k_D can be calculated according to Eq. (6):

$$k_D = 4\pi R D_{AB} N_A \quad (6)$$

where R denotes the reaction distance, N_A is the Avogadro number, and D_{AB} is the mutual diffusion coefficient of the reactants A (•OH) and B (TCS). D_{AB} has been calculated ÅÅfrom D_A and D_B according to the reference (Truhlar, 1985), and D_A and D_B have been estimated from the Stokes–Einstein approach listed in Eq. (7) (Einstein, 1905):

$$D = \frac{k_B T}{6\pi\eta a} \quad (7)$$

where k_B is the Boltzmann constant, T is the temperature, η denotes the viscosity of the solvent (water in our case, $\eta = 8.9 \times 10^{-4}$ Pa s), and a is the radius of the solute.

The half-life ($t_{1/2}$) of the OH-initiated TCS reaction was calculated using the formula $t_{1/2} = \ln 2/(k_{total} \times [\bullet OH])$, where [•OH] is the •OH concentration.

2.3. Risk assessment calculations

The risk assessment of TCS and its transformation products was carried out using the ECOSAR program (ECOSAR, 2013), to estimate the acute and chronic toxicities of the chemicals to three trophic levels of aquatic organisms (green algae, daphnia, and fish). The most conservative effect concentrations are presented here. The acute toxicity is expressed as EC_{50} value (i.e., the concentration at which 50% of green algae are adversely impaired after a 96-h exposure) for the algae and LC_{50} values (i.e., the concentration at which 50% of fish and daphnia die after a 96- and 48-h exposure, respectively) for the fish and daphnia.

3. Results and discussion

3.1. Reactant properties and structures

The optimized structures of both reactants (TCS and •OH) and the TCS carbon atom numbers are shown in Fig. 1. It can be seen that TCS is a chlorinated phenoxyphenol, containing a benzene ring (B), a phenolic ring (P), and three chlorine substituents. TCS has a twisted conformation, with a dihedral angle of 62.18° between the benzene and phenolic rings, caused by the steric effect between the chlorine and hydroxyl ortho-substituents. Therefore, it is impossible for TCS to

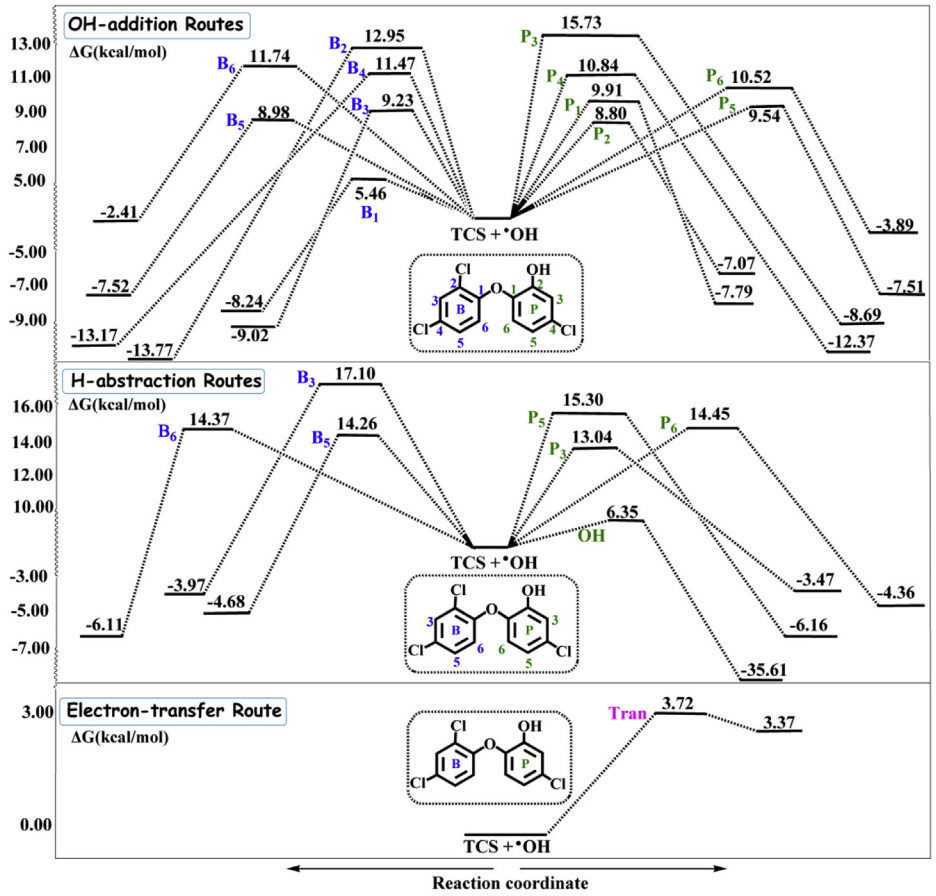

Fig. 2 – Schematic free energy diagram for the reaction between triclosan and •OH at the B3LYP/6-311++G(3df,2p)//B3LYP/6-31+G(d,p) level (kcal mol^{-1}).

present a coplanar conformation, and thus may affect its interactions with target cells to finally lead to the potential toxicity (Song et al., 2011). Although TCS has some different configurations in solid state as reported by Latosińska et al. (2008), the most stable configuration of TCS which is agreement with the detailed study by Özişik et al. (2010) was selected as a model of this compound to consider its fate and transformation mechanism in aquatic environments. Furthermore, it can be seen from Fig. 1, the calculated structural parameters of reactants were reasonably consistent with the available experimental data (given in parentheses) (Latosińska et al., 2012; NIST, 2013). As a result, it can be concluded that the calculated structural parameters for all of the stationary points were reliable at the B3LYP/6-31+G(d,p) level, despite the lack of structural information for some intermediates, transition states, and products.

3.2. *Initial reaction mechanisms and kinetics of TCS with •OH*

3.2.1. *Mechanisms*

Twenty possible TCS reaction routes initiated by •OH were considered and modeled, summarized in Scheme S1a–c, due to its asymmetric TCS structure. For convenience, a nomenclature was established for each route: (i) OH-addition (Scheme S1a) onto C atom of either the benzene ring ($R_{add}B_{1-6}$) or the phenol ring ($R_{add}P_{1-6}$); (ii) H-abstraction (Scheme S1b) from the phenolic hydroxyl group ($R_{abs}OH$) or an H atom of either the benzene ring ($R_{abs}B_{3,5,6}$) or the phenol ring ($R_{abs}P_{3,5,6}$); and (iii) single electron-transfer (Scheme S1c), meaning an electron transfer from TCS by •OH (R_{tran}). The geometries of all of the stationary points such as TSs and products involved in these routes are shown in Figs. S1 and S2.

The potential energy surface for each route is shown in Fig. 2. There was not much variation in the free energy barriers ($\Delta G^{\neq}$s) for the OH-addition routes, except for the lowest and highest $\Delta G^{\neq}$s, which were 5.46 kcal mol^{-1} for the $R_{add}B_1$ route and 15.73 kcal mol^{-1} for the $R_{add}P_3$ route, respectively. For example, the $\Delta G^{\neq}$s were 9.23 kcal mol^{-1} for $R_{add}B_3$, 8.98 kcal mol^{-1} for $R_{add}B_5$, 10.84 kcal mol^{-1} for $R_{add}P_4$, and 10.52 kcal mol^{-1} for $R_{add}P_6$. This indicates that the $R_{add}B_1$ route was the most favorable addition route and the $R_{add}P_3$ route could be ignored. The contributions from the 10 other routes ($R_{add}B_{2-6}$ and $R_{add}P_{1,2,4-6}$) could not be ascertained easily and needed to be calculated from the kinetic viewpoint. The lowest $\Delta G^{\neq}$ for the H-abstraction routes was found to be the $R_{abs}OH$ route ($\Delta G^{\neq} = 6.35$ kcal mol^{-1}), and it was at least nearly 7 kcal mol^{-1} lower than the $\Delta G^{\neq}$ for the other routes ($R_{abs}B_{3,5,6}$ and $R_{abs}P_{3,5,6}$). This implies that H abstraction from the phenolic hydroxyl group by •OH ($R_{abs}OH$) was the almost entirely dominant pathway, leading to the dehydrogenated radical •TCS(−H). The lowest $\Delta G^{\neq}$ (3.72 kcal mol^{-1}) of all of the

OH-initiated TCS reaction routes was found for the electron-transfer route (R_{tran}), but this was the only obtained endergonic route with the reaction energy of 3.37 kcal mol^{-1}. Thus the R_{tran} route was, therefore, less spontaneous than the other routes and could be ruled out from a thermodynamic perspective. The following discussion, about kinetics and toxicity assessments, will, therefore, be focused on the OH-addition and H-abstraction routes.

3.2.2. *Kinetics*

Reaction kinetics studies were carried out, using a temperature range of 273–313 K (Swancutt et al., 2010), to quantitatively evaluate OH-addition and H-abstraction route contributions and to better understand the TCS transformation products in aquatic environments. The rate constants calculated for all of the routes and the overall rate constants (k_{total}; the sum of the rate constants for all of the routes) are given in Table S1. The k_{total} values were 1.08×10^{10}, 1.81×10^{10}, and 2.37×10^{10} $(mol\ L^{-1})^{-1}\ s^{-1}$ at 273, 298, and 313 K, respectively. The data suggested that the OH-initiated TCS reaction was strictly diffusion controlled over the whole temperature range investigated according to the reference (Cramer and Truhlar, 1999). The rate constants for all of the routes and the k_{total} increased with increasing temperature. For example, the rate constants for the $R_{add}B_1$ route increased from 3.58×10^9 to 4.12×10^9 $(mol\ L^{-1})^{-1}\ s^{-1}$ as the temperature increased from 273 to 313 K. Thus, it can be concluded that increasing the temperature promotes the OH-initiated transformation of TCS. However, this slight increase in the rate constant with temperature implies that the reaction was really dependent on diffusion-controlled processes and independent of chemical-reaction-controlled processes.

To estimate the reaction kinetics depended on the temperatures without experimental data, Arrhenius formulae were established for all of the routes within a temperature range of 273–313 K (Table S2). The rate constant, pre-exponential factor, and activation energy for each route could be obtained at a given temperature using these Arrhenius formulae. However, to serve the needs of present work, only the activation energies for the whole reaction of TCS with •OH will be discussed here. The activation energy was found to be only 3.07 kcal mol^{-1} within range of 273–313 K, indicating that the reaction can occur easily and TCS is readily degraded by •OH in aquatic environments.

The $t_{1/2}$ values were calculated for the OH-initiated reactions of TCS between 273 and 313 K (Fig. S3 and Table S3) with 10^{-15}–10^{-18} mol L^{-1} •OH concentrations in natural waters (Brezonik and Fulkerson-Brekken, 1998; Burns et al., 2012). The $t_{1/2}$ was found to be decreased with increasing temperature at a fixed •OH concentration within the investigated temperature range, and the $t_{1/2}$ also decreased with increasing •OH concentration at a fixed temperature. For instance, the $t_{1/2}$ increased from 10.64 h to 443 d as the •OH concentration decreased from 10^{-15} to 10^{-18} mol L^{-1} at 298 K. According to the screening criteria used by the Stockholm Convention (Klasmeier et al., 2005), organic compounds with the $t_{1/2}$ more than 60 d in the aquatic environment were grouped as persistent organic pollutants (POPs)-like compounds. The $t_{1/2}$ for the OH-initiated transformation of TCS in the aquatic environment was above 60 d at •OH concentrations of 1.24×10^{-17}, 7.39×10^{-18}, and 5.64×10^{-18} mol L^{-1} at 273, 298, and 313 K, respectively. So TCS should be considered as a potential POPs-like compound when the •OH concentration is below any of these values at the relevant conditions in the aquatic environment, and it really requires particular attention.

The branching ratio (Γ) dependence of the temperature was calculated to gain an understanding of the contribution of each route to the whole reaction and to quantitatively predict the intermediates formed. Fig. S4a–b shows the Γs for all of the OH-addition and H-abstraction routes, between 273 and 313 K. The Γs for each route, except the $R_{abs}B_1$ and $R_{abs}OH$ routes, increased with increasing temperature. However, the Γs for the $R_{add}B_{2,4,6}$, $R_{add}P_{3,4,6}$, $R_{abs}B_{3,5,6}$, and $R_{abs}P_{3,5,6}$ routes were below 3.6% within the temperature range investigated. For instance, at 298 K, the Γs for the $R_{add}B_{2,4,6}$, $R_{add}P_{3,4,6}$, $R_{abs}B_{3,5,6}$, and $R_{abs}P_{3,5,6}$ routes were below 2.1%. These small Γs suggested that these twelve routes were contributed very less to the OH-initiated transformation of TCS in aquatic environments. For clarity, the Γs dependences of the temperature for the other routes ($R_{add}B_{1,3,5}$, $R_{add}P_{1,2,5}$, and $R_{abs}OH$) are shown in Fig. 3. The Γs for the $R_{abs}OH$ and $R_{add}B_1$ routes at 298 K were 24.8% and 21.7%, respectively, and the other five routes contributed 10.3% ($R_{add}B_3$), 12.5% ($R_{add}B_5$), 4.9% ($R_{add}P_1$), 14.2% ($R_{add}P_2$), and 7.6% ($R_{add}P_5$) to the total rate constant. The $R_{abs}OH$ and $R_{add}B_1$ routes remained the dominant routes with increasing temperature, although the Γs decreased to 20.0% and 17.4%, respectively, at 313 K. Therefore, •TCS(–H) and •TCS–OH_{B1} would be formed as the first main intermediates in the temperature range investigated. However, it is worth noting that the contributions from the five other routes increased to 7.1–13.9% at 313 K (Fig. 3), indicating that their intermediates, •TCS–$OH_{B3,5}$ and •TCS–$OH_{P1,2,5}$, should not be ignored, especially at high temperatures.

3.3. *Subsequent reactions of the primary intermediates*

Based on the results described above, we concluded that six OH-adducts (•TCS–$OH_{B1,3,5}$ and •TCS–$OH_{P1,3,5}$) and a

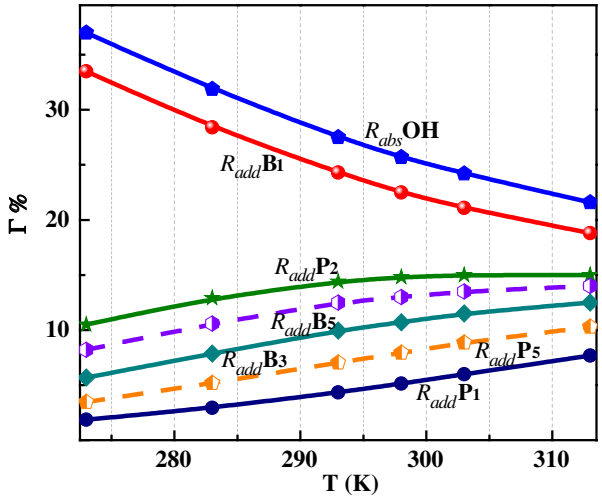

Fig. 3 – Calculated branching ratios (Γ) for the main routes for the reaction between triclosan and •OH between 273 and 313 K.

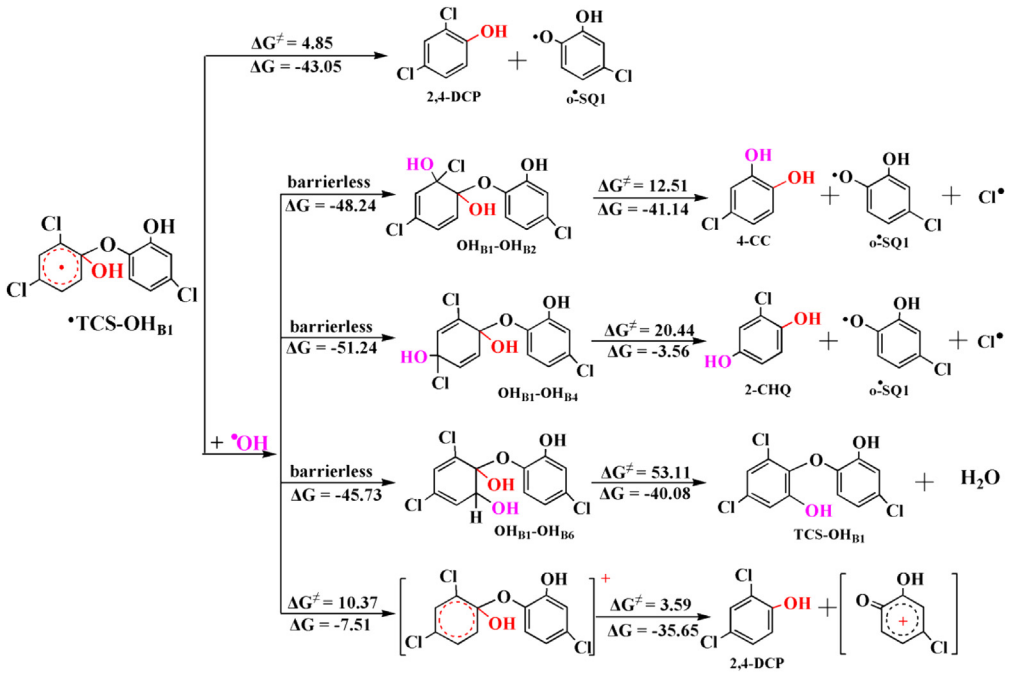

Fig. 4 – Schematic diagram of the •TCS–OH_{B1} routes (kcal mol^{-1}).

dehydrogenated radical (•TCS(–H)) were the main products of the initial reactions of TCS with •OH. These adducts and radicals, being highly active radical species, can undergo a series of subsequent transformation reactions to produce more stable products. So it is very important to track the subsequent reactions of these primary intermediates in the aquatic environment.

3.3.1. *OH-addition products (•TCS–$OH_{B1,3,5}$ and •TCS–$OH_{P1,2,5}$)*

The subsequent degradation routes of •TCS–OH_{B1} are shown in Fig. 4. It can be seen that •TCS–OH_{B1} can undergo ether bond cleavage, by overcoming a $\Delta G^{\neq}$ of 4.85 kcal mol^{-1}, and the main transformation products were 2,4-dichlorophenol (2,4-DCP) and 4-chloro-o-semiquinone (o-•SQ1) at low [•OH]. However, in the presence of enough •OH, •TCS–OH_{B1} is more likely to be attacked by •OH, forming three dihydroxyl-TCS isomers (OH_{B1}–$OH_{B2,4,6}$) but not 2,4-DCP, because these processes are barrier-less, with reaction energies of –48.24, –51.24, and –45.73 kcal mol^{-1}, for OH_{B1}–OH_{B2}, OH_{B1}–OH_{B4}, and OH_{B1}–OH_{B6}, respectively. Subsequently, the ether bond cleavage of OH_{B1}–OH_{B2} and OH_{B1}–OH_{B4} preferentially occurs, forming 4-chlorocatechol (4-CC) ($\Delta G^{\neq}$ = 12.51 and 20.44 kcal mol^{-1}, respectively), while further transformation of OH_{B1}–OH_{B6} is difficult because its $\Delta G^{\neq}$ is high (53.11 kcal mol^{-1}). Similar results were found for the subsequent transformation of •TCS–OH_{P1} (Fig. S5). That is, 4-CC is also the main transformation product at low [•OH], and three dihydroxylated TCS isomers (OH_{P1}–$OH_{P2,4,6}$) can be obtained easily, and then be transformed into final products in the presence of enough •OH.

The subsequent routes for •TCS–OH_{B3} are shown in Fig. S6. It is really difficult routes for example the direct dehydrogenation ($R_{del}H$) and dechlorination ($R_{del}Cl$) in the aquatic environment because of their high $\Delta G^{\neq}$s (33.83 and 43.64 kcal mol^{-1}, respectively) at low [•OH]. However, in the presence of enough •OH, OH-addition to the benzene ring of •TCS–OH_{B3} occurs rapidly through three barrier-less processes with high exothermic energies (ΔG = –48.29, –52.57, and –48.75 kcal mol^{-1}), producing three dihydroxyl-TCS isomers (OH_{B3}–OH_{B2}, OH_{B3}–OH_{B4}, and OH_{B3}–OH_{B6}, respectively). Subsequently, the intermediates, except OH_{B3}–OH_{B6}, can easily form the hydroxylated polychlorinated diphenyl ethers (OH-$PCDE_{1,2}$) via HCl-elimination from OH_{B3}–$OH_{B2,4}$. The single electron transfer route of •TCS–OH_{B3}, mediated by •OH, is also exothermic, and can lead to the formation of the stable monohydroxyl-TCS (TCS–OH_{B3}), with a $\Delta G^{\neq}$ of 6.07 kcal mol^{-1}. Similar conclusions can be drawn for the subsequent transformation routes for •TCS–OH_{B5}, •TCS–OH_{P5}, and •TCS–OH_{P2} (Figs. S7–S9). That is, in the presence of enough •OH, these intermediates would easily be converted into stable hydroxylated products, such as OH_{B5}–$OH_{B2,4,6}$, OH_{P2}–$OH_{B1,3,5}$, and OH_{P5}–$OH_{B2,4,6}$, and then further transformed into monohydroxylated products (TCS–OH_{B5} and TCS–OH_{P5}) and hydroxylated polychlorinated diphenyl ethers (OH-$PCDE_{4,5}$). All of these results were in well agreement with our previous results that TCS is much more easily degraded at high [•OH].

3.3.2. *H-abstraction product •TCS(–H)*

The subsequent transformation routes of •TCS(–H) are shown in Fig. 5. Two possible •TCS(–H) cyclization routes, the $R_{cyc}B_2$ and $R_{cyc}B_6$ routes, could occur at low [•OH]. However, because the $R_{cyc}B_2$ route is endergonic (ΔG = 14.27 kcal mol^{-1}) and the $R_{cyc}B_6$ route is exothermic (ΔG = –1.67 kcal mol^{-1}), the latter route should occur spontaneously. Although the $\Delta G^{\neq}$ of the $R_{cyc}B_6$ route was up to 29.46 kcal mol^{-1}, it was still lower than the energy (35.61 kcal mol^{-1}) released from the original reaction to form •TCS(–H), indicating that the $R_{cyc}B_6$ route should

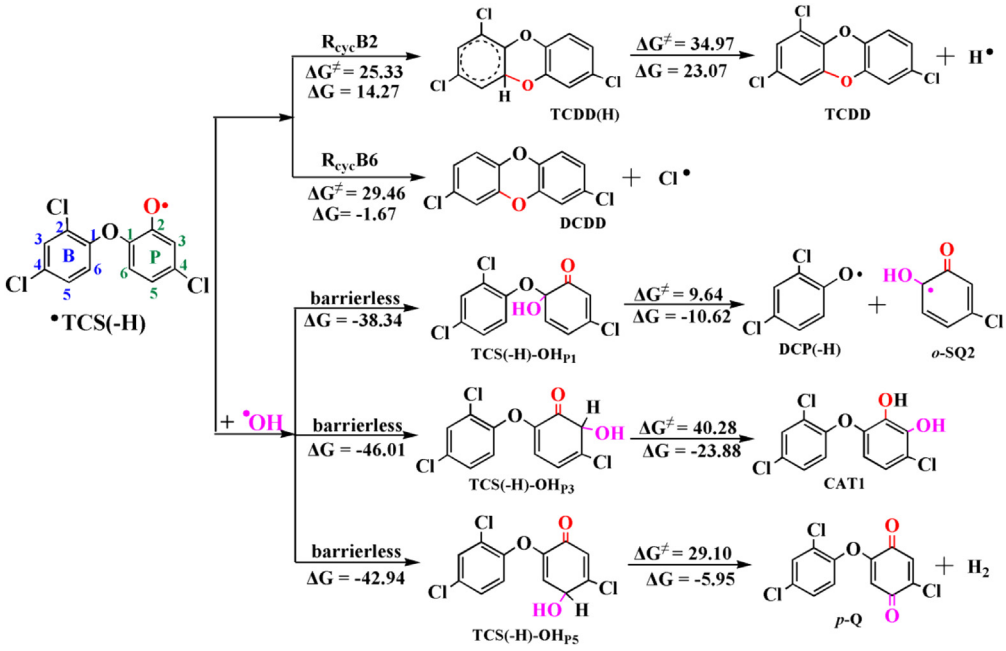

Fig. 5 – Schematic diagram of the •TCS(−H) routes (kcal mol^{-1}).

occur easily, forming dioxins (dichlorodibenzo-*p*-dioxin; DCDD). It is well known that DCDD is an extremely toxic, carcinogenic environmental contaminant. It can, therefore, be confirmed that DCDD could potentially be formed from the OH-initiated transformation of TCS via the intermolecular cyclization of •TCS(−H) in aquatic environments at low [•OH].

However, in the presence of a high [•OH], •TCS(−H) is prone to be further attacked by •OH, to produce three stable OH-adducts (TCS(−H)−$OH_{P1,3,5}$), because these processes are all barrier-less with ΔG values of −38.34, −46.01, and −42.94 kcal mol^{-1}, for TCS(−H)−OH_{P1}, TCS(−H)−OH_{P3}, and TCS(−H)−OH_{P5}, respectively. Subsequently, because of these high ΔG values, TCS(−H)−$OH_{P1,3,5}$ can easily form the corresponding products, with $\Delta G^{\neq}$s of 9.64 (TCS(−H)−OH_{P1}), 40.28 (TCS(−H)−OH_{P3}), and 29.10 (TCS(−H)−OH_{P5}) kcal mol^{-1}, and DCDD will not be observed in aquatic environments at high [•OH]. In addition, because TCS(−H)−OH_{P1} has the lowest $\Delta G^{\neq}$, its product, 2,4-dichlorinated phenoxide radical •DCP(−H), is the main product, and can be converted into the monochlorinated derivative 4-chloro-1,2-benzoquinone (Peller and Kamat, 2005).

In summary, our findings give an insight into TCS transformation mechanisms and kinetics at different [•OH]. Our results showed that the OH-initiated transformation of TCS was a potential source of dioxins in aquatic environments at low [•OH], while the risks from other products produced during the OH-initiated transformation of TCS should not be neglected.

3.4. *Toxicity predictions for the intermediates formed during the transformation of TCS*

3.4.1. *The toxicities of TCS*

Experimental risk assessments of ECs are time consuming, costly, and equipment dependent, so a cost-effective and convenient computational approach was developed for quick toxicity screening. The ECOSAR program has often been used because it is a reliable method for theoretically predicting the toxicities of transformation products (Buth et al., 2007). The acute and chronic toxicities of TCS were first calculated using the ECOSAR program, at three trophic levels (Table S4). The acute toxicity of TCS was estimated as LC_{50} for fish and daphnia as well as EC_{50} for green algae, and these values were 0.48, 0.47, and 1.67 mg L^{-1}, respectively. According to criteria set by the European Union (described in Annex VI of Directive 67/548/EEC), TCS was classed as very toxic to fish and daphnia (LC_{50} < 1.0 mg L^{-1}) and toxic to green algae (1.0 < EC_{50} < 10.0 mg L^{-1}). The calculated toxicities well agreed with experimental values (LC_{50}s for fish and daphnia and an EC_{50} for green algae of 0.37, 0.39, and 1.5 mg L^{-1}, respectively) (Boreen et al., 2003; Raut and Angus, 2010), showing that the ECOSAR program is suitable to assess the toxicities of TCS and its transformational products. The chronic toxicity values (ChVs) for TCS were predicted to be 0.07 mg L^{-1} for fish, 0.09 mg L^{-1} for daphnia, and 0.76 mg L^{-1} for green algae. According to the Chinese hazard evaluation guidelines for new chemical substances (HJ/T 154–2004), TCS was classified as very chronically toxic to fish and daphnia (ChV < 0.1 mg L^{-1}) and chronically toxic to green algae (0.1 < ChV < 1.0 mg L^{-1}). From the point of view of its acute and chronic toxicity, therefore, TCS was found to be a toxic substance that could cause great harm to aquatic organisms at three trophic levels. So the toxicity assessment of TCS transformation products in aquatic environments should be considered seriously.

3.4.2. *The toxicities of intermediates in the OH-addition route*

A schematic representation of the evolution of the acute and chronic toxicities through the $R_{add}B_1$ route is shown in Fig. 6a–f, and the corresponding toxic values are given in Table S5. The LC_{50}s of all of the intermediates (OH_{B1}–$OH_{B2,4,6}$, 4-CC, and 2,4-DCP) for fish were higher than 1.0 mg L^{-1}

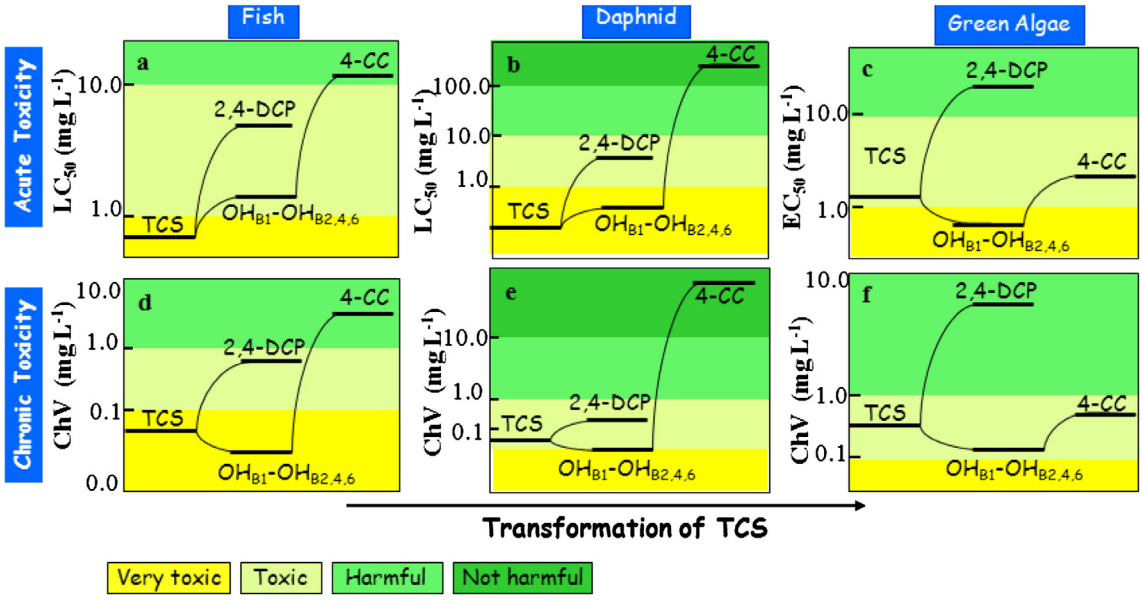

Fig. 6 – Evolution of acute and chronic toxicities through the $R_{add}B_1$ route.

(Fig. 6a), indicating that all of the intermediates were one level less toxic than TCS. That is, although all of these products are acutely toxic to fish, the overall toxicity declined through the $R_{add}B_1$ route relative to TCS. Similar results were obtained for the acute toxicities to daphnia (Fig. 6b). However, the case was somewhat different for the acute toxicities to green algae (Fig. 6c), and the EC_{50}s for OH_{B1}–$OH_{B2,4,6}$ were obtained as 0.03–0.08 mg L^{-1} (Table S5), suggesting that OH_{B1}–$OH_{B2,4,6}$ were one level more toxic than TCS. Furthermore, the final transformation product of OH_{B1}–$OH_{B2,4,6}$, 4-CC (EC_{50} = 3.89 mg L^{-1}) was less toxic to green algae than TCS (EC_{50} = 1.67 mg L^{-1}), although both compounds were at the same toxic level. These results imply that the acute toxicities of the intermediates to green algae initially increased, and then decreased as OH_{B1}–$OH_{B2,4,6}$ was transformed into 4-CC. Similar results can be seen in Fig. 6d–f for the chronic toxicity evolution through the $R_{add}B_1$ route. That is, the chronic toxicity initially increased slightly and then decreased significantly through the transformation processes. The evolutions of the acute and chronic toxicities through the other OH-addition routes ($R_{add}B_{3,5}$,$P_{1,2,5}$) were the same as the $R_{add}B_1$ route (Figs. S10–S14 and Table S6).

3.4.3. *The toxicities of the degradation products through the H-abstraction route*

A schematic representation of the evolutions of the acute and chronic toxicities through the $R_{abs}OH$ route is shown in Fig. S15a–f, and the corresponding toxicities are summarized in Table S7. The LC_{50}s of the products, TCS(–H)–OH_{P1}, TCS(–H)–OH_{P3}, TCS(–H)–OH_{P5}, and DCDD, for fish were found to be 0.81, 0.47, 1.82, and 0.11 mg L^{-1}, respectively. The LC_{50}s for each of the products except DCDD were around or smaller than that of TCS (0.48 mg L^{-1}). From Fig. 5, it can be seen that the acute toxicity to fish would decrease slightly at high [•OH], but it would otherwise increase rapidly through the transformation of TCS into DCDD in aquatic environments at low [•OH] (Fig. S15a). The acute toxicities varied in similar ways for daphnia (Fig. S15b). However, the EC_{50}s of the products for green algae, were 0.11 mg L^{-1} for DCDD, 0.84 mg L^{-1} for TCS(–H)–OH_{P1}, 0.05 mg L^{-1} for TCS(–H)–OH_{P3}, and 0.07 mg L^{-1} for TCS(–H)–OH_{P5}, and these are all lower than that of TCS.

The four H-abstraction route products were more chronically toxic than TCS (Fig. S15d–f). For example, the ChVs of DCDD, TCS(–H)–OH_{P1}, TCS(–H)–OH_{P3}, and TCS(–H)–OH_{P5} for fish were 0.02, 0.01, 0.01, and 0.02 mg L^{-1}, respectively (Table S7), and these are slightly lower than that of TCS (0.07 mg L^{-1}). So we can conclude that the chronic toxicity of the produced products were more toxic than TCS. However, these more toxic intermediates could be further degraded at high [•OH], so the chronic toxicity could be, finally, decreased. Similar toxicity evolutions through the transformation process have been found for other ECs (Fang et al., 2013).

In summary, our results show that TCS is potentially persistent in aquatic environments at low [•OH], so the toxicities of its transformation products need to be assessed, particularly for chronic effects on different aquatic organisms. The accumulation of hazardous products of the OH-initiated transformation of TCS may affect the aquatic environment more seriously than TCS itself, so the OH-initiated transformation of TCS needs to be studied in more depth.

3.5. *TCS fate predictions in AOP systems*

The frequently use and broad application of TCS and its inadequate removal in current wastewater treatment methods mean that high TCS concentrations have been found in wastewater treatment plant effluents. Conventional wastewater treatment approaches do not easily lead to the degradation of TCS by microorganisms, and it may be persistent in aquatic environments, although it could be depleted by OH-initiated reactions, for example in the photochemical transformation. Therefore, AOPs (in which •OH is continuously generated, and the [•OH] can be up to

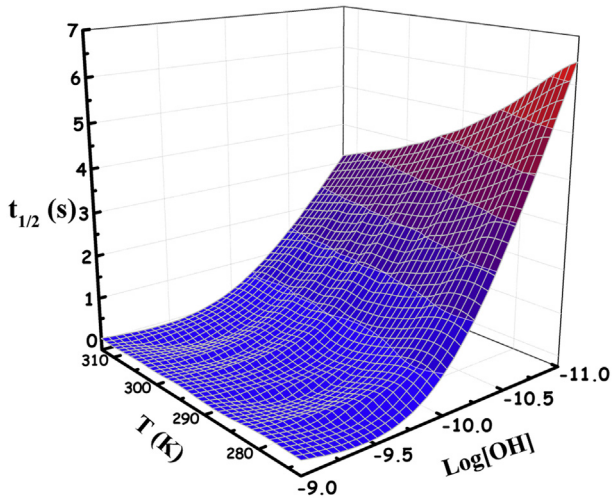

Fig. 7 – Plot of the half-life of the triclosan reaction as a function of the •OH concentrations ([•OH]) and a temperature range of 273–313 K, under AOP conditions.

10^{-9}–10^{-10} mol L^{-1}) can be used as an alternative to the conventional wastewater treatment methods, to eliminate TCS from aquatic environments. That is, [•OH] is 5–9 orders of magnitude higher in an AOP system than that in natural waters (Gong et al., 2011).

To better understand the fate of TCS in AOPs systems, the $t_{1/2}$s were calculated for the OH-initiated reactions of TCS with varying [•OH] and temperature (Fig. 7 and Table S3). The $t_{1/2}$ was predicted to be only 0.40 s at 298 K with a [•OH] of 10^{-10} mol L^{-1}, but the $t_{1/2}$ decreased about ten-fold as the [•OH] increased to 10^{-9} mol L^{-1}. As discussed above, dioxins are unlikely to be formed when •OH is continuously generated in AOPs, which explains why dioxin-type intermediates have not been experimentally observed in AOPs, for example photocatalytic processes (Bokare and Choi, 2011; Rafqah et al., 2006; Song et al., 2012; Yu et al., 2006). These findings suggest that AOPs are very effective and promising technologies to eliminate TCS from drinking water and wastewater, and, importantly, they are environmentally friendly technologies. The $t_{1/2}$s were found to be 0.07–0.65 s at 273 K and 0.03–0.32 s at 313 K in AOPs within a [•OH] range of 10^{-9}–10^{-10} mol L^{-1}, implying that increasing the temperature in an AOP system can decrease the $t_{1/2}$, being more favorable to the degradation of TCS. These theoretical results are expected to be helpful in identifying the actual degradation mechanism(s) for the transformation of TCS in aquatic environments and in assessing the risks associated with the products. The results will also help in the design of further experimental studies and in the industrial application of AOPs.

4. Conclusions

We developed a computational approach to assess the transformation of TCS in aquatic environments and to evaluate the toxicity of the intermediates formed to aquatic organisms. The major findings were:

1) The computational approach is a cost-effective way of revealing the mechanisms and kinetics, and assessing the risks associated with, the transformation of TCS in the aquatic environment;
2) OH-initiated reactions, as a part of the photo-transformation process, play an important role in the transformation of TCS in the natural aquatic environment. The TCS $t_{1/2}$ ranged from 10.64 h to 443 d at 298 K, and, at [•OH] below 7.39×10^{-18} mol L^{-1}, TCS should be considered a potential POP-like compound, requiring particular attention;
3) The [•OH] in the aquatic environment can influence the transformation intermediates. For example, dioxin could be formed through the intermolecular cyclization of the H-abstraction product at low [•OH]. This suggests that the OH-initiated transformation of TCS could be a source of dioxins in natural waters;
4) The acute and chronic toxicities of TCS as well as its transformation products were evaluated at three trophic levels. As TCS was degraded, intermediates that are more toxic than TCS can be produced, so the risk assessment of TCS transformation products in aquatic environments cannot be ignored, particularly relating to chronic effects on different aquatic organisms. The accumulation of hazardous products from the OH-initiated transformation of TCS may have more serious effects on aquatic environments than TCS itself;
5) AOPs are very effective and promising technologies to eliminate TCS from drinking water and wastewater, and dioxins are unlikely to be formed if enough •OH can be continuously generated for example in an AOPs system.

Acknowledgments

This is contribution No. 1744 from GIGCAS. The authors gratefully acknowledge the financial support from Knowledge Innovation Program of Chinese Academy of Sciences (No. KZCX2-YW-QN103), National Nature Science Foundation of China (No. 40973068), Science and Technology R&D Fund of Shenzhen City (JC201005250054A) and of Guangdong Province (2012A032300010), and the Earmarked Fund of the State Key Laboratory of Organic Geochemistry (SKLOG2012A01 and SKLOG2009A02).

Appendix A. Supplementary data

Supplementary data related to this article can be found at http://dx.doi.org/10.1016/j.watres.2013.10.027.

REFERENCES

Allmyr, M., McLachlan, M.S., Sandborgh-Englund, G., Adolfsson-Erici, M., 2006. Determination of triclosan as its pentafluorobenzoyl ester in human plasma and milk using

electron capture negative ionization mass spectrometry. Anal. Chem. 78 (18), 6542–6546.
An, T.C., Yang, H., Li, G.Y., Song, W.H., Cooper, W.J., Nie, X.P., 2010a. Kinetics and mechanism of advanced oxidation processes (AOPs) in degradation of ciprofloxacin in water. Appl. Catal. B-environ. 94 (3–4), 288–294.
An, T.C., Yang, H., Song, W.H., Li, G.Y., Luo, H.Y., Cooper, W.J., 2010b. Mechanistic considerations for the advanced oxidation treatment of fluoroquinolone pharmaceutical compounds using TiO_2 heterogeneous catalysis. J. Phys. Chem. A 114 (7), 2569–2575.
Anger, C.T., Sueper, C., Blumentritt, D.J., McNeill, K., Engstrom, D.R., Arnold, W.A., 2013. Quantification of triclosan, chlorinated triclosan derivatives, and their dioxin photoproducts in lacustrine sediment cores. Environ. Sci. Technol. 47 (4), 1833–1843.
Aranami, K., Readman, J.W., 2007. Photolytic degradation of triclosan in freshwater and seawater. Chemosphere 66 (6), 1052–1056.
Barone, V., Cossi, M., 1998. Quantum calculation of molecular energies and energy gradients in solution by a conductor solvent model. J. Phys. Chem. A 102 (11), 1995–2001.
Bokare, A.D., Choi, W., 2011. Advanced oxidation process based on the Cr(III)/Cr(VI) redox cycle. Environ. Sci. Technol. 45 (21), 9332–9338.
Boreen, A.L., Arnold, W.A., McNeill, K., 2003. Photodegradation of pharmaceuticals in the aquatic environment: a review. Aquat. Sci. 65 (4), 320–341.
Brezonik, P.L., Fulkerson-Brekken, J., 1998. Nitrate-induced photolysis in natural waters: controls on concentrations of hydroxyl radical photo-intermediates by natural scavenging agents. Environ. Sci. Technol. 32 (19), 3004–3010.
Burns, J.M., Cooper, W.J., Ferry, J.L., King, D.W., DiMento, B.P., McNeill, K., Miller, C.J., Miller, W.L., Peake, B.M., Rusak, S.A., Rose, A.L., Waite, T.D., 2012. Methods for reactive oxygen species (ROS) detection in aqueous environments. Aquat. Sci. 74 (4), 683–734.
Buth, J.M., Arnold, W.A., McNeill, K., 2007. Unexpected products and reaction mechanisms of the aqueous chlorination of cimetidine. Environ. Sci. Technol. 41 (17), 6228–6233.
Buxton, G.V., Greenstock, C.L., Helman, W.P., Ross, A.B., 1988. Critical-review of rate constants for reactions of hydrated electrons, hydrogen-atoms and hydroxyl radicals ($^{\bullet}OH/^{\bullet}O^{-}$) in aqueous-solution. J. Phys. Chem. Reference Data 17 (2), 513–886.
Calafat, A.M., Ye, X., Wong, L.Y., Reidy, J.A., Needham, L.L., 2008. Urinary concentrations of triclosan in the US population: 2003–2004. Environ. Health Perspect. 116 (3), 303–307.
Chen, X.J., Richard, J., Liu, Y.L., Dopp, E., Tuerk, J., Bester, K., 2012. Ozonation products of triclosan in advanced wastewater treatment. Water Res. 46 (7), 2247–2256.
Collins, F.C., Kimball, G.E., 1949. Diffusion-controlled reaction rates. J. Colloid Sci. 4 (4), 425–437.
Cramer, C.J., Truhlar, D.G., 1999. Implicit solvation models: equilibria, structure, spectra, and dynamics. Chem. Rev. 99 (8), 2161–2200.
Dong, M.M., Rosario-Ortiz, F.L., 2012. Photochemical formation of hydroxyl radical from effluent organic matter. Environ. Sci. Technol. 46 (7), 3788–3794.
ECOSAR (2013) http://www.epa.gov/oppt/newchems/tools/21ecosar.htm.
Einstein, A., 1905. Über die von der molekularkinetischen Theorie der Wärme geforderte Bewegung von in ruhenden Flüssigkeiten suspendierten Teilchen. Annalen der Physik 322 (8), 549–560.
Evans, M.G., Polanyi, M., 1935. Some applications of the transition state method to the calculation of reaction velocities, especially in solution. Trans. Faraday Soc. 31 (1), 875–893.
Eyring, H., 1935. The activated complex in chemical reactions. J. Chem. Phys. 3 (2), 107–115.
Fair, P.A., Lee, H.B., Adams, J., Darling, C., Pacepavicius, G., Alaee, M., Bossart, G.D., Henry, N., Muir, D., 2009. Occurrence of triclosan in plasma of wild Atlantic bottlenose dolphins (*Tursiops truncatus*) and in their environment. Environ. Pollut. 157 (8–9), 2248–2254.
Fang, H.S., Gao, Y.P., Li, G.Y., An, J.B., Wong, P.K., Fu, H.Y., Yao, S.D., Nie, X.P., An, T.C., 2013. Advanced oxidation kinetics and mechanism of preservative propylparaben degradation in aqueous suspension of TiO_2 and risk assessment of its degradation products. Environ. Sci. Technol. 47 (6), 2704–2712.
Frisch, M.J., Truck, G.W., Schlegel, H.B., Scuseria, G.E., Robb, M.A., Cheeseman, J.R., Zakrzewski, V.G., Montgomery, J.A., Stratmann, J.R.E., Burant, J.C., Dapprich, S., Millam, J.M., Daniels, A.D., Kudin, K.N., Strain, M.C., Farkas, O., Tomasi, J., Barone, V., Cossi, M., Cammi, R., Mennucci, B., Pomelli, C., Adamo, C., Clifford, S., Ochterski, J., Petersson, G.A., Ayala, P.Y., Cui, Q., Morokuma, K., Malick, D.K., Rabuck, A.D., Raghavachari, K., Foresman, J.B., Cioslowski, J., Ortiz, J.V., Boboul, A.G., Stefnov, B.B., Liu, G., Liaschenko, A., Piskorz, P., Komaromi, L., Gomperts, R., Martin, R.L., Fox, D.J., Keith, T., Al–Laham, M.A., Peng, C.Y., Nanayakkara, A., Gonzalez, C., Challacombe, M., Gill, P.M.W., Johnson, B., Chen, W., Wong, M.W., Andres, J.L., Gonzalez, C., Head–Gordon, M., Replogle, E.S., Pople, J.A., 2003. Revision A.1. Guassian, Inc., Pittsburgh, PA. GAUSSIAN 03.
Galano, A., Alvarez-Idaboy, J.R., 2009. Guanosine plus OH radical reaction in aqueous solution: a reinterpretation of the UV-vis data based on thermodynamic and kinetic calculations. Org. Lett. 11 (22), 5114–5117.
Gee, R.H., Charles, A., Taylor, N., Darbre, P.D., 2008. Oestrogenic and androgenic activity of triclosan in breast cancer cells. J. Appl. Toxicol. 28 (1), 78–91.
Geens, T., Neels, H., Covaci, A., 2012. Distribution of bisphenol-A, triclosan and n-nonylphenol in human adipose tissue, liver and brain. Chemosphere 87 (7), 796–802.
Gong, A.S., Lanzl, C.A., Cwiertny, D.M., Walker, S.L., 2011. Lack of influence of extracellular polymeric substances (EPS) level on hydroxyl radical mediated disinfection of *Escherichia coli*. Environ. Sci. Technol. 46 (1), 241–249.
Heidler, J., Halden, R.U., 2007. Mass balance assessment of triclosan removal during conventional sewage treatment. Chemosphere 66 (2), 362–369.
Ishibashi, H., Matsumura, N., Hirano, M., Matsuoka, M., Shiratsuchi, H., Ishibashi, Y., Takao, Y., Arizono, K., 2004. Effects of triclosan on the early life stages and reproduction of medaka *Oryzias latipes* and induction of hepatic vitellogenin. Aquat. Toxicol. 67 (2), 167–179.
Klasmeier, J., Matthies, M., Macleod, M., Fenner, K., Scheringer, M., Stroebe, M., Le Gall, A.C., McKone, T., Van De Meent, D., Wania, F., 2005. Application of multimedia models for screening assessment of long-range transport potential and overall persistence. Environ. Sci. Technol. 40 (1), 53–60.
Kliegman, S., Eustis, S.N., Arnold, W.A., McNeill, K., 2013. Experimental and theoretical insights into the involvement of radicals in triclosan phototransformation. Environ. Sci. Technol. 47 (13), 6756–6767.
Kolpin, D.W., Furlong, E.T., Meyer, M.T., Thurman, E.M., Zaugg, S.D., Barber, L.B., Buxton, H.T., 2002. Pharmaceuticals, hormones, and other organic wastewater contaminants in U.S. streams, 1999–2000: a national reconnaissance. Environ. Sci. Technol. 36 (6), 1202–1211.
Latch, D.E., Packer, J.L., Arnold, W.A., McNeill, K., 2003. Photochemical conversion of triclosan to 2,8-dichlorodibenzo-p-dioxin in aqueous solution. J. Photochem. Photobiol. A-Chem. 158 (1), 63–66.

Latch, D.E., Packer, J.L., Stender, B.L., VanOverbeke, J., Arnold, W.A., McNeill, K., 2005. Aqueous photochemistry of triclosan: formation of 2,4-dichlorophenol, 2,8-dichlorodibenzo-p-dioxin, and oligomerization products. Environ. Toxicol. Chem. 24 (3), 517–525.

Latosińska, J.N., Latosińska, M., Tomczak, M.A., Seliger, J., Žagar, V., Maurin, J.K., 2012. Conformations and intermolecular interactions pattern in solid chloroxylenol and triclosan (API of anti-infective agents and drugs). A 35Cl NQR, 1H-14N NQDR, X-ray and DFT/QTAIM study. Magn. Reson. Chem. 50 (2), 89–105.

Latosińska, J.N., Tomczak, M.A., Kasprzak, J., 2008. Thermal stability and molecular dynamics of triclosan in solid state studied by 35Cl-NQR spectroscopy and DFT calculations. Chem. Phys. Lett. 462 (4–6), 284–288.

Liang, X.M., Nie, X.P., Ying, G.G., An, T.C., Li, K.B., 2013. Assessment of toxic effects of triclosan on the swordtail fish (*Xiphophorus helleri*) by a multi-biomarker approach. Chemosphere 90 (3), 1281–1288.

Marcus, R.A., 1964. Chemical and electrochemical electron-transfer theory. Annu. Rev. Phys. Chem. 15, 155–196.

Marcus, R.A., 1993. Electron transfer reactions in chemistry. Theory and experiment. Rev. Mod. Phys. 65 (3), 599–610.

Marcus, R.A., 1997. Electron transfer reactions in chemistry. Theory and experiment. Pure Appl. Chem. 69 (1), 13–29.

Mezcua, M., Gómez, M.J., Ferrer, I., Aguera, A., Hernando, M.D., Fernández-Alba, A.R., 2004. Evidence of 2,7/2,8-dibenzodichloro-p-dioxin as a photodegradation product of triclosan in water and wastewater samples. Anal. Chim. Acta 524 (1–2), 241–247.

Nelsen, S.F., Blackstock, S.C., Kim, Y., 1987. Estimation of inner shell Marcus terms for amino nitrogen compounds by molecular orbital calculations. J. Am. Chem. Soc. 109 (3), 677–682.

Nelsen, S.F., Weaver, M.N., Pladziewicz, J.R., Ausman, L.K., Jentzsch, T.L., O'Konek, J.J., 2006. Estimation of electronic coupling for intermolecular electron transfer from cross-reaction data. J. Phys. Chem. A 110 (41), 11665–11676.

2013. http://webbook.nist.gov/chemistry/.

Okuno, Y., 1997. Theoretical investigation of the mechanism of the baeyer-villiger reaction in nonpolar solvents. Chem. – A Eur. J. 3 (2), 210–218.

Özişik, H., Bayari, S.H., Sağlam, S., 2010. Conformational and vibrational studies of triclosan. AIP Conf. Proc. 1203 (1), 1227–1232.

Peller, J., Kamat, P.V., 2005. Radiolytic transformations of chlorinated phenols and chlorinated phenoxyacetic acids. J. Phys. Chem. A 109 (42), 9528–9535.

Rafqah, S., Wong-Wah-Chung, P., Nelieu, S., Einhorn, J., Sarakha, M., 2006. Phototransformation of triclosan in the presence of TiO_2 in aqueous suspension: mechanistic approach. Appl. Catal. B-environ. 66 (1–2), 119–125.

Raut, S.A., Angus, R.A., 2010. Triclosan has endocrine-disrupting effects in male western mosquitofish, *Gambusia Affinis*. Environ. Toxicol. Chem. 29 (6), 1287–1291.

Shu, Z.Q., Bolton, J.R., Belosevic, M., El Din, M.G., 2013. Photodegradation of emerging micropollutants using the medium-pressure UV/H_2O_2 advanced oxidation process. Water Res. 47 (8), 2881–2889.

Singer, H., Müller, S., Tixier, C., Pillonel, L., 2002. Triclosan: occurrence and fate of a widely used biocide in the aquatic environment: field measurements in wastewater treatment plants, surface waters, and lake sediments. Environ. Sci. Technol. 36 (23), 4998–5004.

Son, H.S., Ko, G., Zoh, K.D., 2009. Kinetics and mechanism of photolysis and TiO_2 photocatalysis of triclosan. J. Hazard. Mater. 166 (2–3), 954–960.

Song, Y., Ambati, J., Parkin, S., Rankin, S.E., Robertson, L.W., Lehmler, H.J., 2011. Crystal structure and density functional theory studies of toxic quinone metabolites of polychlorinated biphenyls. Chemosphere 85 (3), 386–392.

Song, Z., Wang, N., Zhu, L.H., Huang, A.Z., Zhao, X.R., Tang, H.Q., 2012. Efficient oxidative degradation of triclosan by using an enhanced Fenton-like process. Chem. Eng. J. 198, 379–387.

Swancutt, K.L., Dail, M.K., Mezyk, S.P., Ishida, K.P., 2010. Absolute kinetics and reaction efficiencies of hydroxyl-radical-induced degradation of methyl isothiocyanate (MITC) in different quality waters. Chemosphere 81 (3), 339–344.

Truhlar, D.G., 1985. Nearly encounter-controlled reactions - the equivalence of the steady-state and diffusional viewpoints. J. Chem. Educ. 62 (2), 104–106.

Valters, K., Li, H.X., Alaee, M., D'Sa, I., Marsh, G., Bergman, A., Letcher, R.J., 2005. Polybrominated diphenyl ethers and hydroxylated and methoxylated brominated and chlorinated analogues in the plasma of fish from the Detroit River. Environ. Sci. Technol. 39 (15), 5612–5619.

Vione, D., Falletti, G., Maurino, V., Minero, C., Pelizzetti, E., Malandrino, M., Ajassa, R., Olariu, R.I., Arsene, C., 2006. Sources and sinks of hydroxyl radicals upon irradiation of natural water samples. Environ. Sci. Technol. 40 (12), 3775–3781.

Wenk, J., von Gunten, U., Canonica, S., 2011. Effect of dissolved organic matter on the transformation of contaminants induced by excited triplet states and the hydroxyl radical. Environ. Sci. Technol. 45 (4), 1334–1340.

Wilson, B.A., Smith, V.H., Denoyelles, F., Larive, C.K., 2003. Effects of three pharmaceutical and personal care products on natural freshwater algal assemblages. Environ. Sci. Technol. 37 (9), 1713–1719.

Wong-Wah-Chung, P., Rafqah, S., Voyard, G., Sarakha, M., 2007. Photochemical behaviour of triclosan in aqueous solutions: kinetic and analytical studies. J. Photochem. Photobiol. A-Chem. 191 (2–3), 201–208.

Yang, H., Li, G.Y., An, T.C., Gao, Y.P., Fu, J.M., 2010. Photocatalytic degradation kinetics and mechanism of environmental pharmaceuticals in aqueous suspension of TiO_2: a case of sulfa drugs. Catal. Today 153 (3–4), 200–207.

Yu, J.C., Kwong, T.Y., Luo, Q., Cai, Z.W., 2006. Photocatalytic oxidation of triclosan. Chemosphere 65 (3), 390–399.